This is a pre-print version of the article

S. Curia, D.S.A. De Focatiis and S.M. Howdle (2015), *High-pressure rheological analysis of CO2-induced melting point depression and viscosity reduction of poly(ε-caprolactone)*, Polymer **69**, pp 17–24. DOI: 10.1016/j.polymer.2015.05.026
The post-print can be found at http://dx.doi.org/10.1016/j.polymer.2015.05.026

High-pressure rheological analysis of CO_2-induced melting point depression and viscosity reduction of poly(ε-caprolactone)

S. Curia[a], D.S.A. De Focatiis[b], S.M. Howdle[a*]

[a]University of Nottingham, School of Chemistry, University Park, Nottingham, NG72RD, UK

[b]University of Nottingham, Division of Materials, Mechanics and Structures, Faculty of Engineering, University Park, Nottingham NG72RD , UK

Corresponding author: Tel.: +44 (0)115 951 3486; fax: +44 (0)115 846 8459; email: Steve.Howdle@nottingham.ac.uk

Abstract

High-pressure rheology has been used to assess the effects of supercritical carbon dioxide ($scCO_2$) on the melting point (T_m) and viscosity of poly(ε-caprolactone) (PCL) over a range of temperatures and pressures up to 300 bar over a wide range of shear rates. Plots of the storage modulus and damping factor against temperature show a significant shift of T_m to lower temperatures in the presence of CO_2, indicating that the polymer crystals melt at temperatures much lower than the ambient pressure T_m.

Furthermore, a significant decrease in the viscosity of two PCL grades with different molecular weight (M_n~10 kDa and 80 kDa) was also detected upon increasing the CO_2 pressure to 300 bar. Experimental viscosity data were fitted to the Carreau model to quantify the extent of the plasticising effects on the zero-shear viscosity and relaxation time under different conditions.

Similar analyses were conducted under high-pressure nitrogen, to compare the effects obtained in the presence of a non-plasticising gas.

Keywords: poly(ε-caprolactone), supercritical CO_2, rheology, melting, viscosity, Carreau.

1. Introduction

In recent years there has been increasing interest in the use of high-pressure CO_2 as a reaction medium or plasticiser for polymer synthesis and processing [1-6]. CO_2 has been exploited as a solvent for polymerisations [7, 8], as a foaming agent [1, 9-13], for precipitation/separation [14], particle formation [15, 16] and encapsulation [17].

High-pressure CO_2 is able to plasticise and effectively liquefy many polymers at temperatures below their glass transition temperatures (T_g) and melting points (T_m) [2, 16, 18-27], thereby opening up opportunities for new processes and incorporation of thermally labile molecules [17, 28]. The CO_2-induced plasticisation mimics the effect of heating the polymer and it is characterised by an increased segmental and chain mobility [29]: the CO_2 molecules exhibit significant specific interactions with many polymers, mainly due to their large quadrupole moment [5, 30]. These interactions often results in high sorption levels and decrease the intermolecular bonding between the chains [31]. This causes an increase in the free volume fraction (v_f) and therefore a higher mobility of the polymer chains, hence leading to a decrease in viscosity with the CO_2 molecules acting as molecular lubricants [16, 31].

Furthermore, the plasticisation is easily reversible: upon depressurisation, the supercritical solvent is removed and no residue is left. This use of CO_2 can be extremely valuable in the preparation of polymeric materials for food packaging and medical applications [16, 29]. This, together with the accessible critical point of CO_2 (31.1 °C and 73.8 bar) and its non-flammability, non-toxicity and low price, make CO_2 a valuable renewable alternative to conventional solvents for polymer synthesis and processing.

PCL is a hydrophobic biodegradable polyester used in a wide range of applications such as food packaging, engineering materials and adhesives [32-36]. It is a semi-crystalline polyester with T_m ~ 55-70 °C and T_g ~ -60 °C that can be synthesised through ring-opening polymerisation of ε-caprolactone (ε-CL) using catalysts such as stannous octanoate or enzymes such as Candida Antarctica Lipase B [37, 38].

The degradation of PCL occurs through the hydrolysis of its ester linkages under physiological conditions [37]. For this reason, PCL has also received much attention for use as an implantable, resorbable material and is already used in many medical applications such as drug delivery, sutures, dentistry and tissue engineering [9, 12, 37, 39, 40].

Nonetheless, molten PCL requires the use of high temperatures (above 140 °C) in order to achieve suitably low viscosities for melt-processing [41]. These conditions are not acceptable for most medical applications where bioactive molecules are incorporated into the polymer, since these can be easily damaged by the high temperature. Lower temperature processing can be achieved by the use of organic solvents, but this introduces unwelcome residues and can inactivate complex biomolecules [42]. In addition, the use of solvents imposes the need for an often challenging purification step for their removal after processing, thus making the overall process longer and more expensive.

The ability of CO_2 to be absorbed into PCL has been previously shown [43]. A change in the morphology of the polymer under CO_2 was also observed by Kelly et al.through infrared (IR) analysis by monitoring the carbonyl peak at 1720 cm^{-1} [44], and a decrease in the reptation time in the presence of high-pressure CO_2 was also found by the same group [45]. The plasticisation of this polymer under CO_2 was also studied optically [46, 47] and through high-pressure calorimetry [48].

In addition, the diffusivity, solubility and specific volume of PCL/CO_2 solutions have been recently studied by coupling gravimetric and spectroscopic techniques [49, 50]. There is no doubt that high-pressure studies for the development and optimisation of CO_2–assisted polymer processing techniques are topical and timely [3].

However, in the current literature there is a lack of any direct study of the loss and storage moduli as a function of temperature and pressure, and hence of the T_m of PCL in CO_2 through high-pressure rheological analysis. Therefore, we have investigated the use of high-pressure rheology to detect the melting point of PCL under CO_2 (1-120 bar) by conducting an oscillatory rheometric study under high-pressure conditions. Furthermore, only few shear viscosity data over a narrow shear rate range are available for PCL in the presence of $scCO_2$ [51]. Hence, the aims of this study are to measure the T_m depression of PCL through direct monitoring of the polymer viscoelasticity under CO_2, and to study the effects of compressed CO_2 and N_2 on the shear viscosities of two grades of PCL of different molar mass (10 kDa and 80 kDa) under various temperature and pressure conditions, over a wide range of shear rates. These data will contribute to the understanding of the structural state of semi-crystalline polyesters in the presence of $scCO_2$, and will aid the development of lower temperature melt processes of such polymers.

2. Materials and methods

2.1 Materials

PCL flakes (PCL10) with a density of 1.15 g/mL at 25 °C, M_n ~10 kDa and M_w ~14 kDa (by GPC) and PCL beads (PCL80) with a density of 1.15 g/mL at 25 °C, M_n ~80 kDa and M_w ~94 kDa (by GPC) were purchased from Sigma Aldrich (UK). The polymers were ground to obtain a powder before use. Supercritical Fluid Chromatography (SFC) grade 4.0 CO_2 (minimum purity 99.99%) and N_2 (99%) were purchased from BOC Special Gases (UK) and used as received.

2.2 Methods

2.2.1 T_m depression analysis

The effect of CO_2 on the T_m of PCL10 was studied using a Physica MCR301 rheometer (Anton Paar, Austria) equipped with Peltier temperature controller and a high-pressure cell (parallel plate geometry with 20 mm diameter and a 1 mm gap disc; PP20/Pr) with an upper operating pressure of 150 bar at room temperature and a maximum temperature of 300 °C. In a typical experiment 700 mg of polymer powder were added to the cup of the rheometer. A preliminary temperature ramp to 80 °C at 10 °C min^{-1}, followed by 5 minutes isothermal, was carried out to obtain a solid polymer disk upon cooling to 20 °C at 10 °C min^{-1}. Three preliminary strain amplitude sweeps at 1 Hz at ambient pressure were performed on the disk to identify a strain value within the linear viscoelastic region (LVR), and mean values are shown in **Figure 1**. From these data, a strain amplitude of 1% was identified as suitable and well within the LVR.

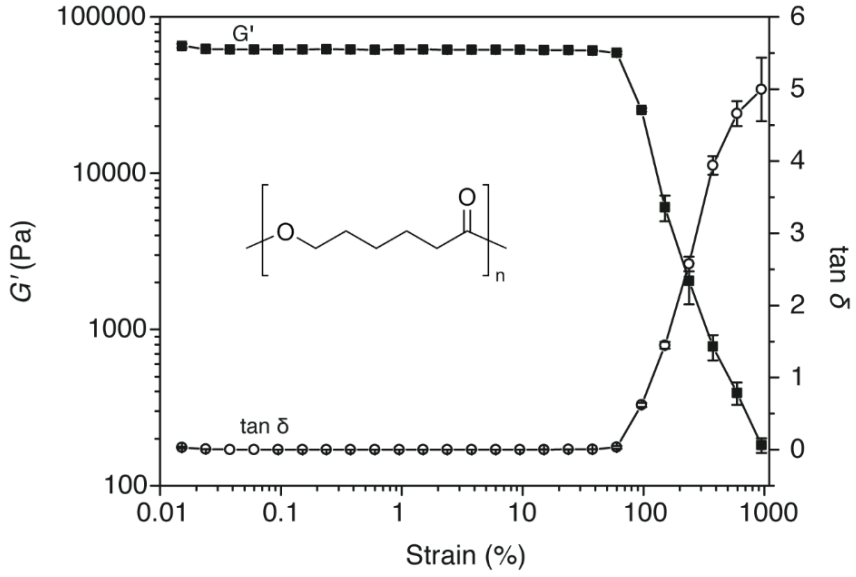

Figure 1. Strain amplitude sweep showing the storage modulus, *G′,* and loss tangent, tan *δ,* as a function of strain for PCL10 at ambient pressure and 20 °C at 1 Hz. The point at which the *G′* and tan *δ* start to deviate from the plateau values indicates departure from linear viscoelastic behaviour. For this reason, the oscillatory tests were conducted at 1 Hz with a strain amplitude of 1%. The polymer structure is shown (inset).

The cell was then sealed and CO_2 was added using a syringe pump (Teledyne Isco 260D, USA). After pressurisation, the polymer was left to soak at 20 °C for 50 minutes to allow for CO_2 diffusion. A time study showed that longer times did not result in significant further drops in the T_m, see Supporting Information (SI) (**Figure S1-S4**). The temperature of the cell was increased at a rate of 5 °C min^{-1} whilst imposing an oscillating strain of 1% to the sample at 1 Hz. Throughout the temperature scans the syringe remained connected to the cell to maintain the required pressure during heating. The shear storage modulus, G', and the loss modulus, G'', were recorded as a function of temperature. The T_m was taken as the temperature at which G'' is a maximum. All the experiments were repeated three times to give data confidence.

2.2.2 Shear viscosity high-pressure analyses

High-pressure steady state rheometric studies (*i.e.* continuous shearing at different selected shear rates) were carried out on PCL10 and PCL80 using an Anton Paar MCR 102 rheometer equipped a Teledyne Isco 260D syringe pump and with a 400 bar cell electrically heated (parallel plate geometry, PP20/Pr). The instrument was calibrated with mineral oils of standard viscosity supplied by Anton Paar.

The polymer powder was inserted in the cup and a preliminary temperature sequence was performed to melt the polymer. The sample was then allowed to equilibrate at 80 °C and the system sealed and pressurised. Samples were left for 50 minutes at pressure to soak. The rotation experiments were performed at constant temperature with logarithmically increasing shear rate over a 2 minute period, from 10^{-3} to 10^{3} s^{-1} for PCL80, and from 1 to 10^{3} s^{-1} for PCL10. Due to the structural limits given by the ball-bearings in the pressure cell, the minimum torque that could be applied with our system was 200 µN.m. When applying the minimum torque to two different liquids, the resulting minimum shear rate will be lower in the higher viscosity material. For this reason, measurements carried out on low viscosity materials start at higher shear rates.

A matching set of experiments were carried out under N_2 at 60, 120 and 180 bar, by connecting a cylinder directly to the rheometer inlet through high-pressure Swagelok® tubing.

All steady state experiments were repeated at least three times; the mean values ± 1 standard deviation are shown in the figures.

Temperature studies at ambient pressure and under CO_2 (at 120 bar) were conducted on PCL10 ($\dot{g}$ =12.0 s^{-1}) and PCL80 ($\dot{g}$=0.1 s^{-1}) by increasing the temperature from 80 °C to 180 °C in 20 °C steps at 5 °C/min. After each ramp, a dwell period of 10 minutes was imposed in order for the sample to reach thermal equilibrium before the collection of 5 measurements, and then ramping to the next temperature.

Finally, transient shear experiments studies (time-dependent viscosity at constant applied shear rates, ranging from 0.25 s^{-1} to 5 s^{-1}) were conducted on PCL80 at ambient pressure (80 and 120 °C) and under CO_2 (80 °C, 120 bar) to investigate whether any phase separation and/or changes of solubility arise during shearing. Measurements of viscosity are plotted against time (**Figure S6 and S7)**. Due to the low viscosity and the equipment low torque limit the same analysis could not be carried out on PCL10.

2.2.3 View cell plasticisation study

In order to observe visually the effect of CO_2 on the physical state of PCL10, a fixed volume view cell (100 mL) was used [52]. This view cell was manufactured in-house from 316-stainless steel with two thick sapphire windows located at the two ends of the cylindrical body which houses the inlet and outlet pipes.

In a typical experiment, 200 mg of sample were added in a glass vial and inserted in the view cell. The windows were sealed and clamped to the body, and CO_2 was added up to 50 bar. The temperature was raised to the desired value. When the temperature was stable, the CO_2 pressure was increased to the required value.

2.2.4 Differential Scanning Calorimetry (DSC)

DSC analyses on PCL10 were performed using a TA-Q2000 DSC (TA Instruments, USA) calibrated with sapphire and indium standards. In a standard experiment, the sample (6.00 ± 0.10 mg) was melted with a first heating scan up to 80 °C and cooled down to 20 °C (10 °C/min). A second heating scan, with the same temperature ramp settings of the oscillatory rheological analyses (80 °C; 5 °C/min) was then carried out. Between each ramp, a 5-minute isotherm was imposed.

The T_m was determined from the maximum of the endothermic peak, and the degree of crystallinity (X_c) was calculated from

$$X_c = \frac{\Delta H_f(T_m)}{\Delta H_f^0(T_m^0)} \qquad (1)$$

where $\Delta H_f(T_m)$ is the measured enthalpy of fusion and $\Delta H_f^0(T_m^0)$ is the enthalpy of fusion of fully crystalline PCL, taken as 135.44 J g^{-1} [53-56]. The T_m as measured from DSC analysis is (64.6 ± 0.2) °C, whilst the X_c is (51.7 ± 0.5) %.

3. Results and Discussion

3.1 Effect of pressure on T_m of PCL10

Typical oscillatory rheometric data obtained for PCL10 at ambient pressure show two distinct regions (**Figure 2**): at lower temperatures G' has a value of ~60 kPa, typical of PCL above its T_g but below its T_m [57]. With increasing temperature there is a steep drop in the value of G' to ~2 kPa, as the material undergoes a thermal transition to a viscous fluid. There is an associated peak in G'' at the same temperature. This transition is associated with the melting of crystal spherulites in the polymer. The T_m at atmospheric pressure, as measured by rheology, is therefore 68.1 ± 0.6 °C, in good agreement with T_m reported elsewhere in the literature [37, 45] and with that measured by DSC in this work (64.6 ± 0.2 °C).

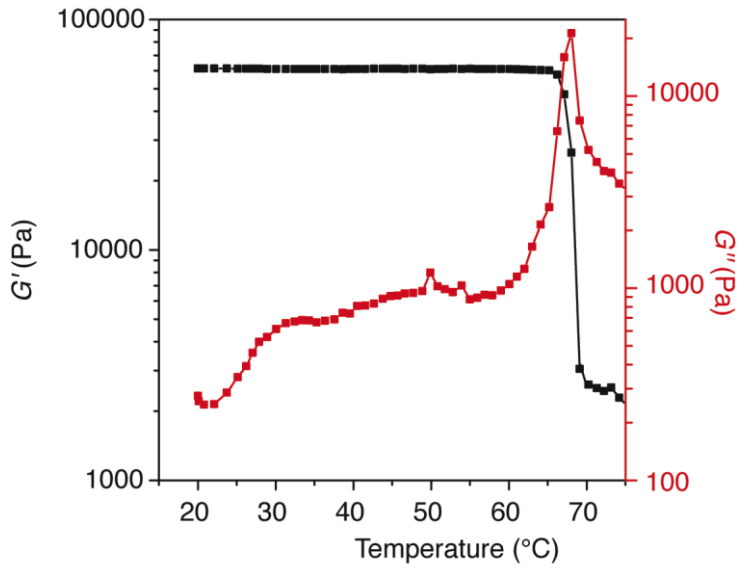

Figure 2. Oscillatory rheometric measurements of G' and G'' as a function of temperature for PCL10 at ambient pressure. The dramatic changes in G' and G'' are produced by the melting of the polymer crystals. The average T_m obtained from the peak in G'' is (68.1 ± 0.6) °C.

The same experiment was performed over a range of pressures to evaluate the effect of high-pressure CO_2 on the T_m of PCL10. G' (**Figure 3**) and G'' (**Figure 4**) show a strong dependence upon temperature and CO_2 pressures. As expected, the shapes of the curves are similar to those obtained at ambient pressure. However, a comparison between the curves shows that the G' drop and G'' peak, and hence the T_m, are shifted to lower temperatures in the presence of pressurised CO_2.

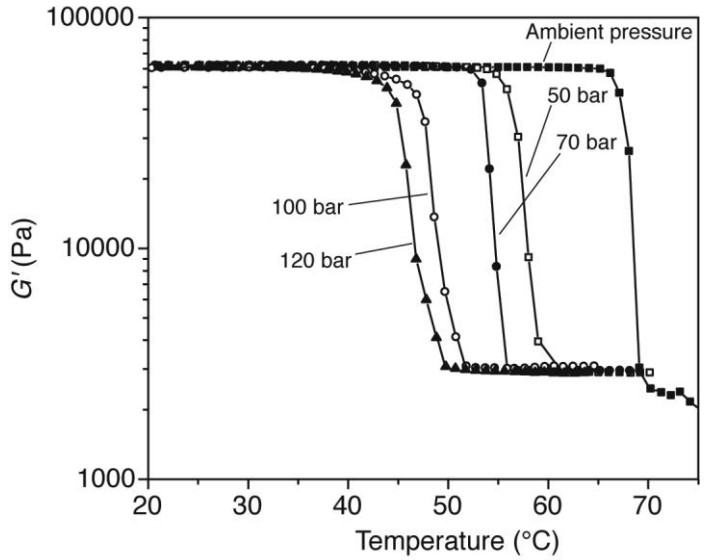

Figure 3. Oscillatory rheometric measurements of *G´* as a function of temperature for PCL10 at a range of CO_2 pressures. The rapid decrease in *G´*is indicative of the polymer melting. Under high-pressure CO_2 the drop is shifted to lower temperatures, thus indicating a significant reduction in the T_m of the polymer (from 68.1 °C to 45.8 °C).

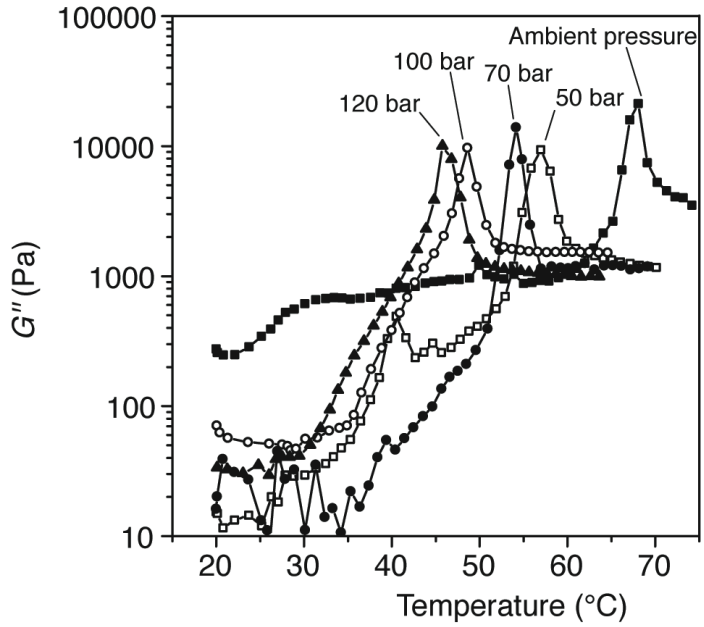

Figure 4. Oscillatory rheometric measurements of *G´´* as a function of temperature for PCL10 at a range of CO_2 pressures. The peak in *G´´* is indicative of the polymer melting. Under CO_2 a significant reduction in the T_m of the polymer is observed.

This is a powerful demonstration of the ability of CO_2 to act as a temporary plasticiser for PCL, by diffusing into the polymer and interacting through Lewis acid/base interactions with the carbonyl groups of the backbone. As a result, the intermolecular interactions are weakened and the polymer can melt at temperatures much lower than the ambient pressure melting point.

The melting points measured from the peaks in G'' under high-pressure CO_2 have been plotted in Figure 5 as a function of pressure. The data show a high correlation (R^2>0.99) linear decrease with increasing pressure, moving from 68.1 °C at atmospheric conditions through to a significantly lower value of 45.8 °C under CO_2 at 120 bar. The data are in good agreement with two literature studies measuring the drop in T_m by DSC [48] and FTIR [44], also shown in Figure 5.

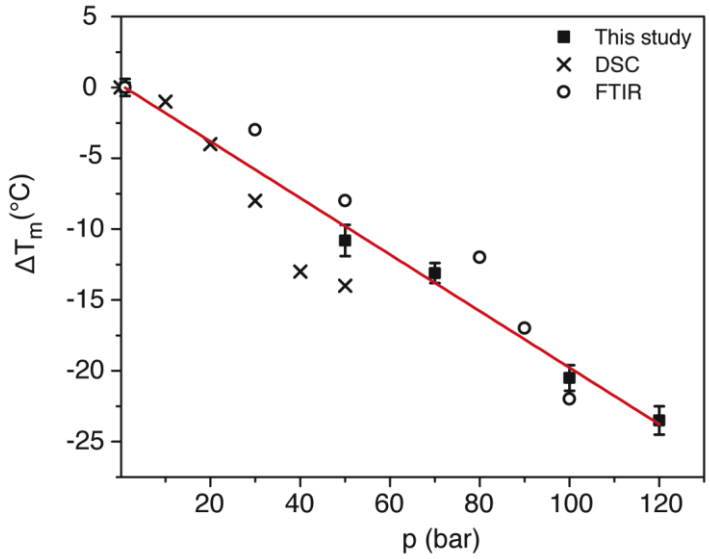

Figure 5. Effect of CO_2 pressure on the change in T_m relative to atmospheric conditions, of PCL10 measured from the peak in G''. The results of this study follow a linear trend with high correlation (R^2>0.99). The data are in good agreement with the results obtained by other research groups through DSC [48] and FTIR [44].

Images from a view cell study (**Figure 6**) clearly show that PCL10 initially appeared as a white powder (a), but in presence of CO_2 at 45 °C and 120 bar was gradually plasticised. The view cell

also confirmed the need for a long soaking time: after 15 minutes the sample was not fully plasticised (b), whilst after 50 minutes no solid residue could be observed (c). This rather long soaking time is most probably due to the high crystallinity of PCL10 (around 52% by DSC). It is well known that CO_2 is able to diffuse and dissolve only in the amorphous regions of polymers [5, 18, 58], and that the T_m depression is given by both polymer-CO_2 interactions in the amorphous regions and crystallites characteristics (*e.g.* lamellar thickness and heat of fusion per unit of volume); hence, different effects will be expected for different levels of amorphous fractions [18, 58].

Images from an additional view cell experiment carried out under high-pressure subcritical CO_2 can be found in the SI (**Figure S5**).

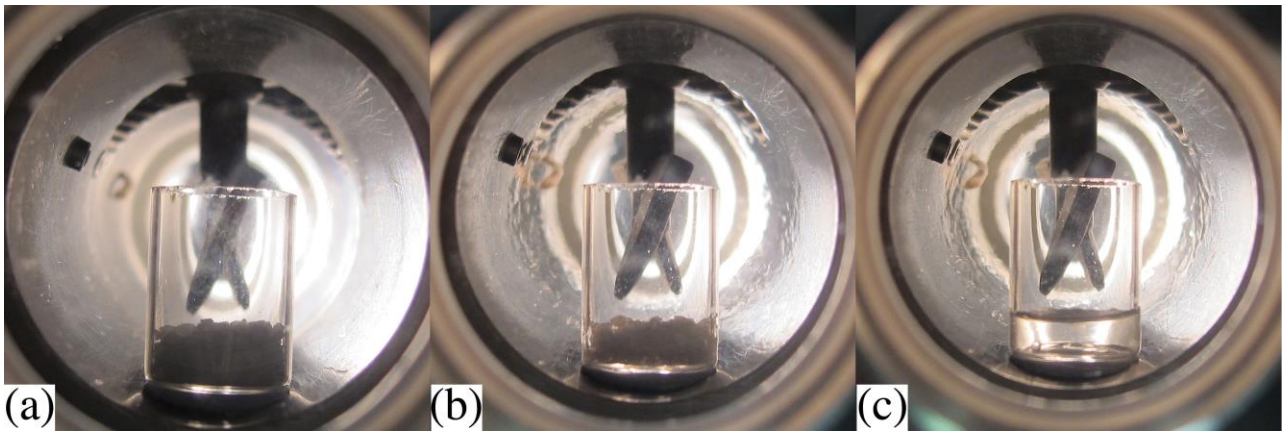

Figure 6. Transitions observed for PCL10 in the view cell experiment: (a) initial polymer in the form of a white powder (room temperature and pressure); (b) sample not completely plasticised after 15 minutes (45 °C, 120 bar); (c) polymer fully plasticised after 50 minutes (45 °C, 120 bar). Although the mechanical stirrer is visible in the images, in these experiments the sample was not stirred.

3.2 Effect of pressure and molecular weight on the viscosity of PCL

Transient shear rheometric experiments were performed at 80 °C on two PCL samples with different molecular weight, PCL10 and PCL80 (M_n ~10 kDa and ~80 kDa respectively) at a range of CO_2 pressures after 50 minutes soaking. The experiments were repeated under N_2, a non-

plasticising gas, up to 180 bar, to gain a better understanding of plasticisation and compression effects. Data in the shear rate region between 10^{-3}-10^{3} s^{-1} was obtained for PCL80. For PCL10, which is of lower molecular weight, and hence of lower viscosity, such low shear rates could not be investigated due to experimental limitations.

The measurements of viscosity as a function of shear rate at 80 °C at a range of CO_2 pressures for PCL10 shown in **Figure 7** exhibit Newtonian behaviour at low shear rates, followed by a shear-thinning region at shear rates above ~300 s^{-1}. The zero shear viscosity is dramatically decreased under CO_2, in agreement with results obtained on other polymers such as amorphous poly(lactic acid) [31], poly(ethylene glycol) [19], and poly(dimethylsiloxane) [59]. At pressures above 120 bar the shear thinning region was less detectable in this shear rate range. became less . This is due to a decrease in the relaxation time of the polymer (higher chain mobility), which results in an extended Newtonian plateau [31]. The critical shear rate at the onset of shear thinning ($\dot{g}_{cr}$) is, in fact, inversely proportional to the relaxation time [60-63]

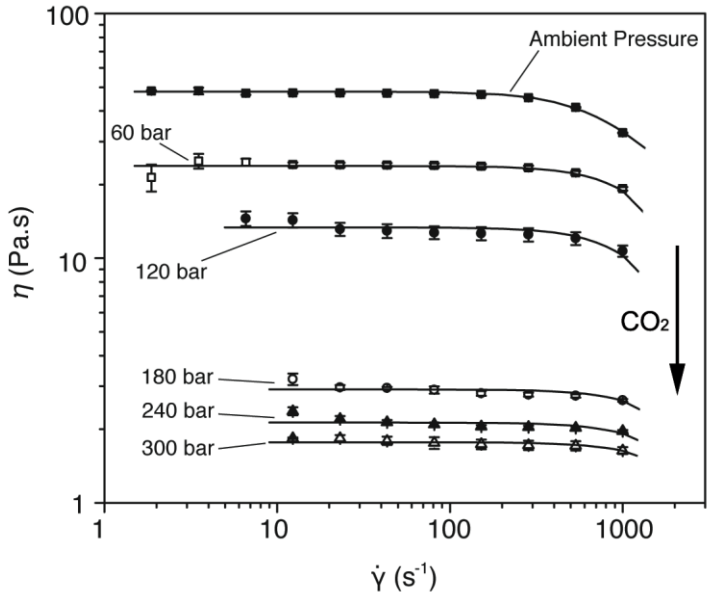

Figure 7. Measurements of steady state shear viscosity of PCL10 (T = 80 °C) at ambient pressure and under increasing CO_2 pressures. A significant reduction in the viscosity is observed with rising CO_2 pressure. The Carreau model (solid lines) is fitted to the data (R^2 > 0.99 for all the fits).

The viscosity data were fitted to the Carreau model to enable quantitative determination of the relaxation time and of the zero shear viscosity. The model is given by:

$$h(\dot{g}) = h_0[1+(l\dot{g})^2]^{-P} \quad (2)$$

where $\eta(\dot{g})$ (Pa.s) is the viscosity at a given shear rate $\dot{g}$ (s^{-1}), η_0 (Pa.s) is the zero shear viscosity, λ (s) is the relaxation time of the polymer and P is the Carreau exponent [31, 64].

Measurements of viscosity as a function of shear rate at 80 °C at a range of N_2 pressures for PCL10 display a small but noticeable increase in viscosity with pressure (**Figure 8**). Also, no significant changes in the extent of the zero shear plateau (hence, in $\dot{g}_{cr}$) were observed, and shear thinning behaviour was always clearly observed within the shear rate range.

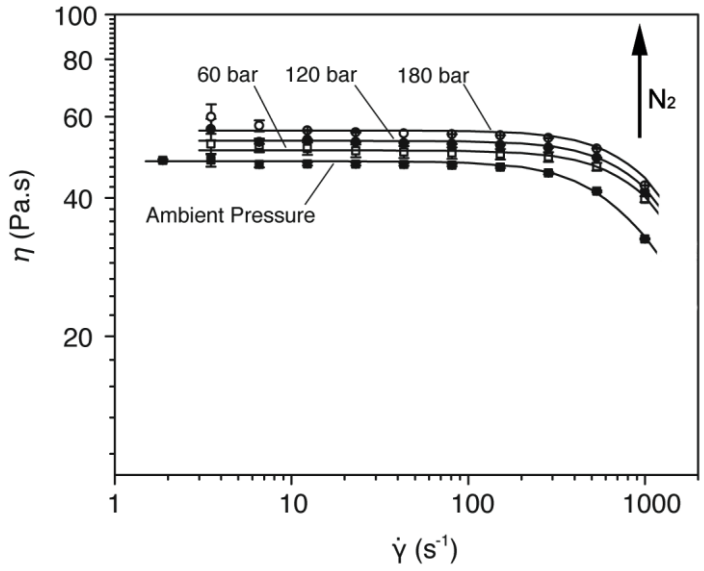

Figure 8. Measurements of steady state shear viscosity of PCL10 (T = 80 °C) at ambient pressure and under increasing N_2 pressures. A small increase in the viscosity is observed with increasing N_2 pressure. The Carreau model (solid lines) is fitted to the data (R^2 > 0.99 for all the sets of data).

The ability of $scCO_2$ to plasticise higher MW PCL was confirmed by viscosity studies carried out on PCL80 (**Figure 9).** The measurements of viscosity as a function of shear rate at 80 °C at a range of CO_2 pressures for PCL80 clearly show that this polymer has a much higher viscosity than PCL10, as expected from the higher degree of chain entanglement [60, 65, 66]. Also, $\dot{g}_{cr}$ is considerably reduced. This is due to the longer relaxation time given by the increased chain length [60-63]. Nonetheless, a dramatic effect of the pressurised CO_2 on the viscosity was observed also for this higher MW polymer.

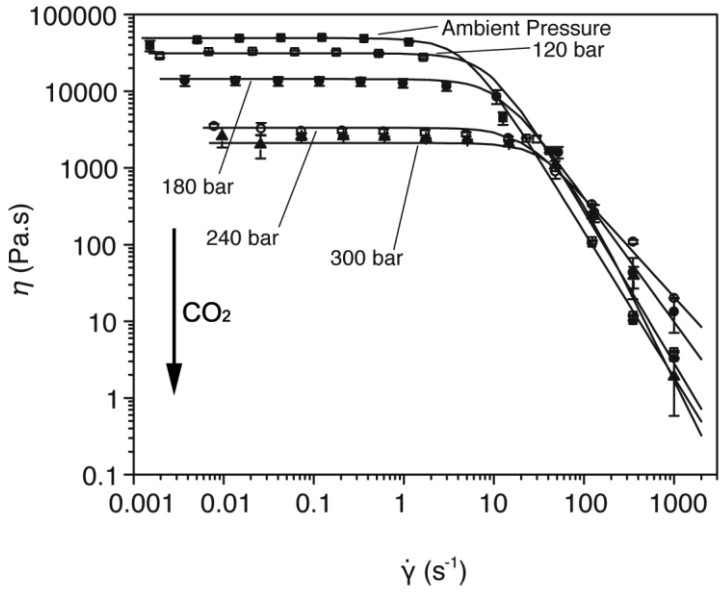

Figure 9. Measurements of transient shear viscosity of PCL80 (T = 80 °C) at ambient pressure and under increasing CO_2 pressures. A significant reduction in the viscosity is observed with rising pressure. The Carreau model (solid lines) is fitted to the data (R^2>0.99 for all the fittings).

The zero shear viscosity is again significantly reduced with increasing CO_2 pressure, and the viscosity reduction is particularly significant in the shear rate region typical of polymer processing (between 1 and 4 s^{-1}) [62, 67]. As expected, increasing CO_2 pressure results in higher $\dot{g}_{cr}$ values, and therefore in reduced relaxation times.

Table 1 shows a comparison of the viscosities of the two polymers at representative shear rates in the Newtonian plateau at ambient pressure, η_0^{amb}, and when plasticised by 300 bar CO_2, $\eta_0^{300\,bar\,CO_2}$. Viscosities are reduced by around 95% for both polymers as a result of the plasticising effect.

Table 1. High-pressure CO_2-induced viscosity reduction of PCL10 and PCL80 in the Newtonian plateau at 80 °C.

M_n (kDa)	$\dot{g}$ (s^{-1})	η_0^{amb} (Pa.s)	$\eta_0^{300\,bar\,CO_2}$ (Pa.s)	η_0 reduction (%)
10	12.0	47.37 ± 0.40	1.84 ± 0.01	96.1
80	0.1	50005.00 ± 429.19	2590.50 ± 280.79	94.8

Transient shear rheometry was carried out also for PCL80 in the presence of high-pressure N_2 (**Figure 10**). Here again no viscosity decrease or changes in the extent of the Newtonian plateau could be observed. The zero shear viscosity increases with increasing pressure, although the effect is small.

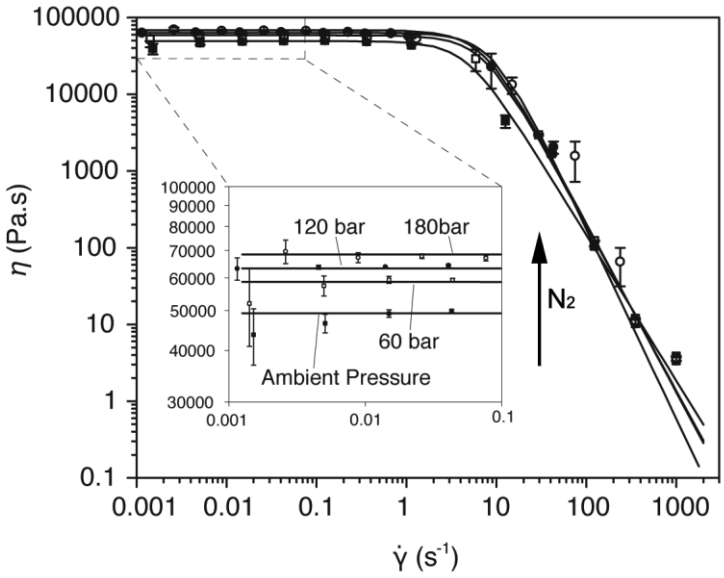

Figure 10. Measurements of transient shear viscosity of PCL80 (T = 80 °C) at ambient pressure and under increasing N_2 pressures. A small increase in the zero shear viscosity is observed with rising pressure (zoomed in region). The Carreau model (solid lines) is fitted to the data (R^2>0.99 for all the fittings).

The zero shear viscosities, calculated from the Carreau model fits for both polymers under CO_2 and N_2, have been plotted as a function of pressure (**Figure 11**). A trend of increasing viscosity with pressure is found under N_2, and of decreasing viscosity with pressure under CO_2. Our data show that the pressure effects in the presence of N_2 give a viscosity increase in good agreement with the Barus equation

$$\eta_0(p) = \eta_0^{\text{atm}} e^{ap} \qquad (3)$$

where $\eta_0(p)$ (Pa.s) is the viscosity at pressure p (Pa), η_0^{atm} (Pa.s) is the viscosity at atmospheric pressure and a (Pa^{-1}) is a pressure-viscosity coefficient [68]. The viscosity reduction with CO_2 pressure would require a negative pressure-viscosity coefficient in order to fit the Barus equation, but the quality of fit would be reduced as the reduction in log viscosity is not linear.

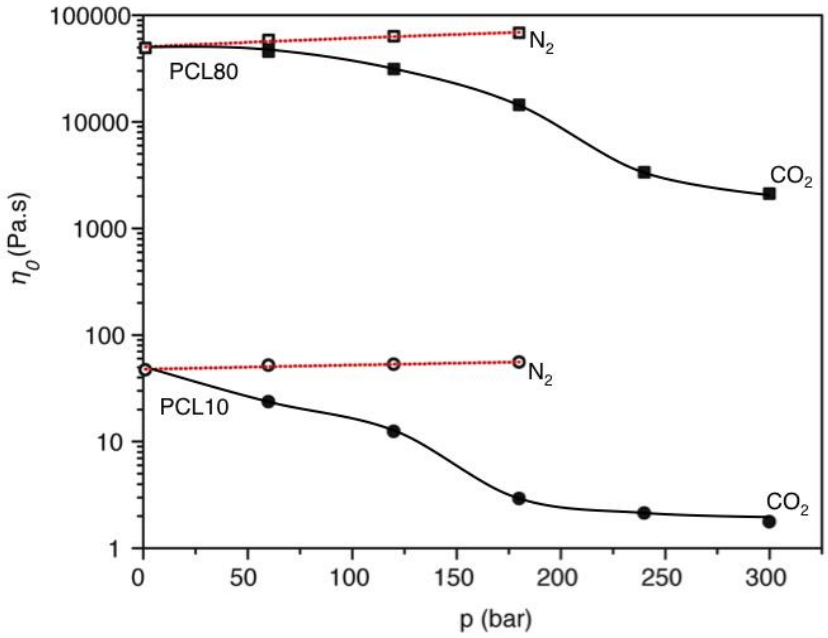

Figure 11. Zero shear viscosity of PCL10 and PCL80 (T=80 °C) under CO_2 and N_2. A small increase in the zero shear viscosity is observed on raising the N_2 pressure (empty symbols), whilst a decrease is seen under CO_2 (black symbols). The data collected under N_2 were fitted to the Barus equation (red dotted lines) with high correlation (R^2>0.99 for all the fittings). Black solid lines connecting the CO_2 data are a guide to the eye.

As stated before, the CO_2 plasticisation also results in a change in the relaxation time of the polymer, which is given by the higher chain mobility. In PCL80 a decrease in relaxation time with CO_2 pressure was recorded (**Figure 12**). However, in PCL10 a decrease with a clear trend could not be observed. It is postulated that in the latter case the polymer chains are not sufficiently entangled because of their low MW, and therefore that the effect of plasticisation from the CO_2 may be less noticeable. A similar result has been observed with increasing temperature for poly(lactic acid) by Kelly *et al.* [31] who observed that at sufficiently high temperatures (well above T_g) no changes in relaxation time could be observed upon the addition of CO_2.

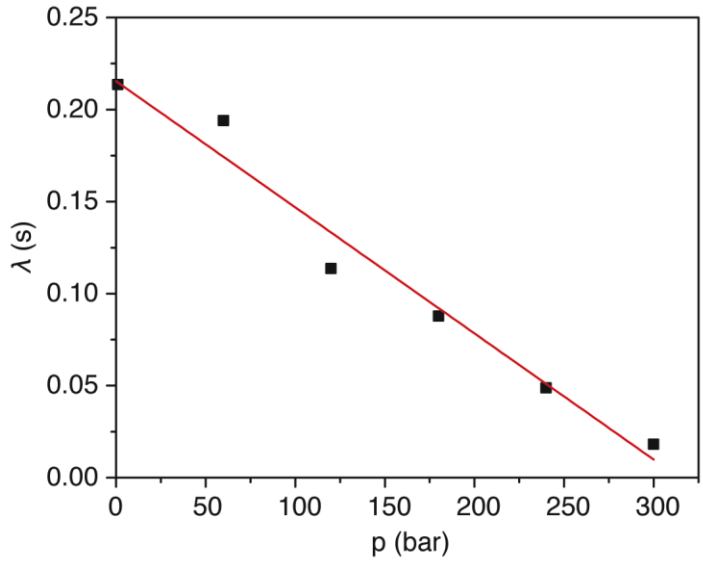

Figure 12. Relaxation time as a function of CO_2 pressure obtained from Carreau model fits for PCL80 at T = 80 °C. A linear decrease (R^2 > 0.96) is observed.

A final set of experiments were conducted at ambient pressure and under CO_2 (120 bar) over a temperature range of 80 to 180 °C in order to correlate the CO_2-induced viscosity depression to the temperature-induced reduction, and in order to obtain activation energies with and without pressurised CO_2 (E_a) (**Table 2**).

The zero shear viscosities of PCL10 ($\dot{g}$ =12.0 s^{-1}) and PCL80 ($\dot{g}$=0.1 s^{-1}) are shown as a function of temperature in an Arrhenius plot (**Figure 13**).

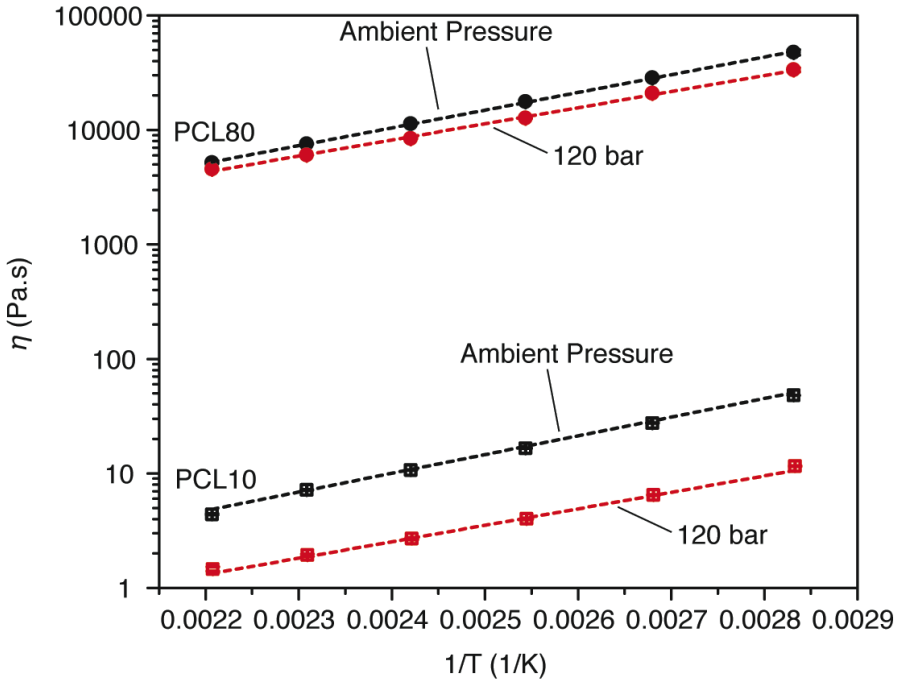

Figure 13. Arrhenius plot of zero shear viscosity as a function of temperature for PCL10 and PCL80 at ambient pressure and under CO_2 (120 bar). In PCL10, a 91% reduction in the viscosity is obtained between 80 °C and 180 °C, whilst an 88% reduction is observed for PCL80 in the same temperature range. The data were fitted to an Arrhenius equation ($R^2 > 0.99$).

Table 2. E_a reduction for PCL under CO_2.

MW	E_a (kJ/mol)		Reduction
(kDa)	Ambient	120 bar	(%)
80	29.59 ± 0.20	26.96 ± 0.18	8.9
10	31.27 ± 0.67	27.50 ± 0.35	12.1

As expected, the fittings show that the E_a of the polymer is reduced under CO_2 (**Table 2**). Furthermore, the data show the dramatic effect of processing with CO_2. For example, for PCL10, processing at 240 bar of CO_2 at 80 °C results in a viscosity (~3 Pa.s) which is equivalent to processing at 180 °C at ambient pressure conditions. For PCL80, exposure to 240 bar of CO_2 at

80 °C produces a viscosity (~3 kPa.s) which is even lower than the ambient pressure viscosity obtained at 180 °C (~6 kPa.s). Therefore, these measurements demonstrate the significant opportunities that high-pressure CO_2 processing of polymers could deliver in terms of energy saving and processing of thermally labile materials [17].

Conclusions

High-pressure rheology was employed to demonstrate clearly the ability of CO_2 to plasticise PCL at supercritical and even sub-critical (60 bar) conditions at 80 °C. For the first time, interpretation of the viscoelastic moduli with temperature plots have been used to show that by adding CO_2 it is possible to lower the melting point of PCL by more than 20 °C (from 68.1 to 45.8 °C). This provides a rheological viewpoint to the CO_2-induced T_m depression of this polymer that correlates well with previous studies using DSC and IR spectroscopy, and a linear drop in T_m with increasing CO_2 pressure was observed.

The viscosity of PCLs of different molecular weights decreased significantly when pressurised CO_2 was added. The reductions observed at 80 °C and 120 bar CO_2 are comparable to those achieved at 180 °C and ambient pressure. A 96% decrease in viscosity relative to ambient pressure was achieved for the 10 kDa polymer, whilst a 95% reduction was obtained for the 80 kDa polymer. The Carreau model was employed for determination of the zero shear viscosity and the relaxation time, both of which decreased with increasing CO_2 pressure. By contrast, the effect of a non-plasticising gas, N_2, was to increase the zero shear viscosity.

In this paper we demonstrated the use of a high-pressure rheometer to detect the T_m depression of polymers under CO_2, highlighting the ability of CO_2 to act as a green and efficient temporary plasticiser that allows for processing of degradable polymers at significantly lower temperatures (80 °C rather than 180 °C).

Acknowledgements: The research leading to these results has received funding from the People Programme (Marie Curie Actions) of the European Union's Seventh Framework Programme FP7/2007-2013/ under REA grants agreement No. [289253].

Abbreviations

CL	-	Caprolactone
DSC	-	Differential scanning calorimetry
E_a	-	Activation energy for viscous flow
IR	-	Infrared
MW	-	Molecular Weight
PCL	-	Poly(ε-caprolactone)
$scCO_2$	-	Supercritical carbon dioxide
SI	-	Supporting information
T_g	-	Glass transition temperature
T_m	-	Melting point
X_c	-	Degree of crystallinity

References

[1] C. Tsioptsias, M.K. Paraskevopoulos, D. Christofilos, P. Andrieux, C. Panayiotou, Polymeric hydrogels and supercritical fluids: The mechanism of hydrogel foaming, Polymer, 52 (2011) 2819-2826.

[2] C. Gutiérrez, M.T. Garcia, S. Curia, S.M. Howdle, J.F. Rodriguez, The effect of CO2 on the viscosity of polystyrene/limonene solutions, The Journal of Supercritical Fluids, 88 (2014) 26-37.

[3] F. Picchioni, Supercritical carbon dioxide and polymers: an interplay of science and technology, Polymer International, (2014) n/a-n/a.

[4] J. Jennings, M. Beija, J.T. Kennon, H. Willcock, R.K. O'Reilly, S. Rimmer, S.M. Howdle, Advantages of Block Copolymer Synthesis by RAFT-Controlled Dispersion Polymerization in Supercritical Carbon Dioxide, Macromolecules, 46 (2013) 6843-6851.

[5] O.R. Davies, A.L. Lewis, M.J. Whitaker, H. Tai, K.M. Shakesheff, S.M. Howdle, Applications of supercritical CO2 in the fabrication of polymer systems for drug delivery and tissue engineering, Advanced drug delivery reviews, 60 (2008) 373-387.

[6] F. Yang, M. Manitiu, R. Kriegel, R.M. Kannan, Structure, permeability, and rheology of supercritical CO2 dispersed polystyrene-clay nanocomposites, Polymer, 55 (2014) 3915-3924.

[7] L. Du, J.Y. Kelly, G.W. Roberts, J.M. DeSimone, Fluoropolymer synthesis in supercritical carbon dioxide, The Journal of Supercritical Fluids, 47 (2009) 447-457.

[8] J. Jennings, M. Beija, A.P. Richez, S.D. Cooper, P.E. Mignot, K.J. Thurecht, K.S. Jack, S.M. Howdle, One-pot synthesis of block copolymers in supercritical carbon dioxide: a simple versatile route to nanostructured microparticles, Journal of the American Chemical Society, 134 (2012) 4772-4781.

[9] I. Tsivintzelis, E. Pavlidou, C. Panayiotou, Biodegradable polymer foams prepared with supercritical CO2–ethanol mixtures as blowing agents, The Journal of Supercritical Fluids, 42 (2007) 265-272.

[10] L. Monnereau, L. Urbanczyk, J.-M. Thomassin, T. Pardoen, C. Bailly, I. Huynen, C. Jérôme, C. Detrembleur, Gradient foaming of polycarbonate/carbon nanotube based nanocomposites with supercritical carbon dioxide and their EMI shielding performances, Polymer, 59 (2015) 117-123.

[11] L. Monnereau, L. Urbanczyk, J.-M. Thomassin, M. Alexandre, C. Jérôme, I. Huynen, C. Bailly, C. Detrembleur, Supercritical CO2 and polycarbonate based nanocomposites: A critical issue for foaming, Polymer, 55 (2014) 2422-2431.

[12] M.J. Jenkins, K.L. Harrison, M.M.C.G. Silva, M.J. Whitaker, K.M. Shakesheff, S.M. Howdle, Characterisation of microcellular foams produced from semi-crystalline PCL using supercritical carbon dioxide, European Polymer Journal, 42 (2006) 3145-3151.

[13] C. Gualandi, L.J. White, L. Chen, R.A. Gross, K.M. Shakesheff, S.M. Howdle, M. Scandola, Scaffold for tissue engineering fabricated by non-isothermal supercritical carbon dioxide foaming of a highly crystalline polyester, Acta biomaterialia, 6 (2010) 130-136.

[14] B. Bungert, G. Sadowski, W. Arlt, Supercritical antisolvent fractionation: measurements in the systems monodisperse and bidisperse polystyrenecyclohexanecarbon dioxide, Fluid Phase Equilibria, 139 (1997) 349-359.

[15] S.P. Nalawade, F. Picchioni, L.P.B.M. Janssen, Batch production of micron size particles from poly(ethylene glycol) using supercritical CO2 as a processing solvent, Chemical Engineering Science, 62 (2007) 1712-1720.

[16] C.A. Kelly, A. Naylor, L. Illum, K.M. Shakesheff, S.M. Howdle, Supercritical CO2: A Clean and Low Temperature Approach to Blending PDLLA and PEG, Advanced Functional Materials, 22 (2012) 1684-1691.

[17] S.M. Howdle, M.S. Watson, M.J. Whitaker, M.C. Davies, K.M. Shakesheff, V.K. Popov, F.S. Mandel, J.D. Wang, Supercritical fluid mixing: preparation of thermally sensitive polymer composites containing bioactive materials, Chemical Communications, (2001) 109-110.

[18] Z. Zhang, Y.P. Handa, CO2-Assisted Melting of Semicrystalline Polymers, Macromolecules, 30 (1997) 8505-8507.

[19] D. Gourgouillon, H.M.N.T. Avelino, J.M.N.A. Fareleira, M. Nunes da Ponte, Simultaneous viscosity and density measurement of supercritical CO2-saturated PEG 400, The Journal of Supercritical Fluids, 13 (1998) 177-185.

[20] P. Alessi, A. Cortesi, I. Kikic, F. Vecchione, Plasticization of Polymers with Supercritical Carbon Dioxide: Experimental Determination of Glass-Transition Temperatures, Journal of Applied Polymer Science, 88 (2002) 2189-2193.

[21] S.A.E. Boyer, J.P.E. Grolier, Modification of the glass transitions of polymers by high-pressure gas solubility, Pure and Applied Chemistry, 77 (2005) 593-603.

[22] M. Lee, C. Tzoganakis, C.B. Park, Extrusion of PE/PS blends with supercritical carbon dioxide, Polymer Engineering & Science, 38 (1998) 1112-1120.

[23] Z. Zhang, Y.P. Handa, An in-situ study of plasticization of polymers by high-pressure gases, Journal of Polymer Science Part B: Polymer Physics, 36 (1998) 977-983.

[24] J.M.D.S. Joseph R. Royer, Saad A. Khan, High-Pressure Rheology and Viscoelastic Scaling Predictions of Polymer Melts Containing Liquid and Supercritical Carbon Dioxide, Journal of Polymer Science Part B: Polymer Physics, 39 (2001) 3055-3066.

[25] R. Pini, G. Storti, M. Mazzotti, H. Tai, K.M. Shakesheff, S.M. Howdle, Sorption and swelling of poly(DL-lactic acid) and poly(lactic-co-glycolic acid) in supercritical CO2: An experimental and modeling study, Journal of Polymer Science Part B: Polymer Physics, 46 (2008) 483-496.

[26] L. Yu, H. Liu, L. Chen, Thermal behaviors of polystyrene plasticized with compressed carbon dioxide in a sealed system, Polymer Engineering & Science, 49 (2009) 1800-1805.

[27] M. Iguchi, Y. Hiraga, K. Kasuya, T.M. Aida, M. Watanabe, Y. Sato, R.L. Smith, Viscosity and density of poly(ethylene glycol) and its solution with carbon dioxide at 353.2K and 373.2K at pressures up to 15MPa, The Journal of Supercritical Fluids, 97 (2015) 63-73.

[28] P.J. Ginty, J.J.A. Barry, L.J. White, S.M. Howdle, K.M. Shakesheff, Controlling protein release from scaffolds using polymer blends and composites, European Journal of Pharmaceutics and Biopharmaceutics, 68 (2008) 82-89.

[29] S.G. Kazarian, Polymer Processing with Supercritical Fluids, Polymer Science Series C, 42 (2000) 78-101.

[30] A.I. Cooper, Polymer synthesis and processing using supercritical carbon dioxide, Journal of Materials Chemistry, 10 (2000) 207-234.

[31] C.A. Kelly, S.M. Howdle, K.M. Shakesheff, M.J. Jenkins, G.A. Leeke, Viscosity studies of poly(DL-lactic acid) in supercritical CO2, Journal of Polymer Science Part B: Polymer Physics, 50 (2012) 1383-1393.

[32] M.F. Koenig, S.J. Huang, Biodegradable blends and composites of polycaprolactone and starch derivatives, Polymer, 36 (1995) 1877-1882.

[33] S. Mecham, A. Sentman, M. Sambasivam, Amphiphilic silicone copolymers for pressure sensitive adhesive applications, Journal of Applied Polymer Science, 116 (2010) 3265-3270.

[34] S. Ebnesajjad, Plastic Films in Food Packaging: Materials, Technology and Applications, Elsevier Science, 2012.

[35] S. Alix, A. Mahieu, C. Terrie, J. Soulestin, E. Gerault, M.G.J. Feuilloley, R. Gattin, V. Edon, T. Ait-Younes, N. Leblanc, Active pseudo-multilayered films from polycaprolactone and starch based matrix for food-packaging applications, European Polymer Journal, 49 (2013) 1234-1242.

[36] A. Munoz-Bonilla, M.L. Cerrada, M. Fernandez-Garcia, A. Kubacka, M. Ferrer, M. Fernandez-Garcia, Biodegradable polycaprolactone-titania nanocomposites: preparation,

characterization and antimicrobial properties, International journal of molecular sciences, 14 (2013) 9249-9266.

[37] M.A. Woodruff, D.W. Hutmacher, The return of a forgotten polymer—Polycaprolactone in the 21st century, Progress in Polymer Science, 35 (2010) 1217-1256.

[38] F.C. Loeker, C.J. Duxbury, R. Kumar, W. Gao, R.A. Gross, S.M. Howdle, Enzyme-Catalyzed Ring-Opening Polymerization of epsilon-Caprolactone in Supercritical Carbon Dioxide, Macromolecules, 37 (2004) 2450-2453.

[39] Q. Xu, X. Ren, Y. Chang, J. Wang, L. Yu, K. Dean, Generation of microcellular biodegradable polycaprolactone foams in supercritical carbon dioxide, Journal of Applied Polymer Science, 94 (2004) 593-597.

[40] M.A. Fanovich, P. Jaeger, Sorption and diffusion of compressed carbon dioxide in polycaprolactone for the development of porous scaffolds, Materials Science and Engineering: C, 32 (2012) 961-968.

[41] B. Kapoor, M. Bhattacharya, Transient shear and extensional properties of biodegradable polycaprolactone, Polymer Engineering & Science, 39 (1999) 676-687.

[42] K. Fu, A.M. Klibanov, R. Langer, Protein stability in controlled-release systems, Nature Biotechnology, 18 (2000) 24-25.

[43] J.C. Gary Leeke, Mike Jenkins, Solubility of Supercritical Carbon Dioxide in Polycaprolactone (CAPA 6800) at 313 and 333 K, Journal of Chemical & Engineering Data, 51 (2006) 1877-1879.

[44] C.A. Kelly, K.L. Harrison, G.A. Leeke, M.J. Jenkins, Detection of melting point depression and crystallization of polycaprolactone (PCL) in scCO2 by infrared spectroscopy, Polym J, 45 (2013) 188-192.

[45] C.A. Kelly, S.H. Murphy, G.A. Leeke, S.M. Howdle, K.M. Shakesheff, M.J. Jenkins, Rheological studies of polycaprolactone in supercritical CO2, European Polymer Journal, 49 (2013) 464-470.

[46] Z. Lian, S.A. Epstein, C.W. Blenk, A.D. Shine, Carbon dioxide-induced melting point depression of biodegradable semicrystalline polymers, The Journal of Supercritical Fluids, 39 (2006) 107-117.

[47] Z. Lian, A.D. Shine, Thermodynamic and Fluid Dynamic Study of the Polymer Liquefaction by Using Supercritical Solvation (PLUSS) Process, Polymeric Materials: Science & Engineering, 93 (2005) 890-891.

[48] S. Murphy, Melting point depression in biodegradable polyesters, in: School of Engineering, Department of Metallurgy and Materials, University of Birmingham, 2011, pp. 100.

[49] M.G. Pastore Carbone, E. Di Maio, G. Scherillo, G. Mensitieri, S. Iannace, Solubility, mutual diffusivity, specific volume and interfacial tension of molten PCL/CO2 solutions by a fully experimental procedure: effect of pressure and temperature, The Journal of Supercritical Fluids, 67 (2012) 131-138.

[50] M.G. Pastore Carbone, E. Di Maio, P. Musto, A. Braeuer, G. Mensitieri, On the unexpected non-monotonic profile of specific volume observed in PCL/CO2 solutions, Polymer, 56 (2015) 252-255.

[51] E. Di Maio, S. Iannace, G. Mensitieri, L. Nicolais, A predictive approach based on the Simha–Somcynsky free-volume theory for the effect of dissolved gas on viscosity and glass transition temperature of polymeric mixtures, Journal of Polymer Science Part B: Polymer Physics, 44 (2006) 1863-1873.

[52] P. Licence, M.P. Dellar, R.G.M. Wilson, P.A. Fields, D. Litchfield, H.M. Woods, M. Poliakoff, S.M. Howdle, Large-aperture variable-volume view cell for the determination of phase-

equilibria in high pressure systems and supercritical fluids, Review of Scientific Instruments, 75 (2004) 3233-3236.

[53] V. Crescenzi, G. Manzini, G. Calzolari, C. Borri, Thermodynamics of fusion of poly- β -propiolactone and poly-ϵ-caprolactone. comparative analysis of the melting of aliphatic polylactone and polyester chains, European Polymer Journal, 8 (1972) 449-463.

[54] F.B. Khambatta, F. Warner, T. Russell, R.S. Stein, Small-angle x-ray and light scattering studies of the morphology of blends of poly(ϵ-caprolactone) with poly(vinyl chloride), Journal of Polymer Science: Polymer Physics Edition, 14 (1976) 1391-1424.

[55] J. Wang, M.K. Cheung, Y. Mi, Miscibility and morphology in crystalline:amorphous blends of polycaprolactone):poly4-vinylphenol) as studied by DSC, FTIR, and 13C solid state NMR, Polymer, 43 (2002) 1357-1364.

[56] H. Ikeda, Y. Ohguma, S. Nojima, Composition Dependence of Crystallization Behavior Observed in Crystalline-Crystalline Diblock Copolymers, Polymer Journal, 40 (2008) 241-248.

[57] K.P. Menard, Dynamic mechanical analysis : a practical introduction / Kevin P. Menard, CRC Press, 2008.

[58] Y.P. Handa, Z. Zhiyi;, W. Betty, Effect of Compressed CO2 on Phase Transitions and Polymorphism in Syndiotactic Polystyrene, Macromolecules, 30 (1997) 8499-8504.

[59] L.J. Gerhardt, A. Garg, C.W. Manke, E. Gulari, Concentration-dependent viscoelastic scaling models for polydimethysiloxane melts with dissolved carbon dioxide, Journal of Polymer Science Part B: Polymer Physics, 36 (1998) 1911-1918.

[60] R.B. Bird, R.C. Armstrong, O. Hassager, Dynamics of polymeric liquids. Vol. 1, 2nd Ed. : Fluid mechanics, 1987.

[61] G.M. Swallowe, Mechanical properties and testing of polymers : an A-Z reference / edited by G.M. Swallowe, Kluwer Academic, 1999.

[62] C.I. Chung, Extrusion of Polymers: Theory and Practice, Hanser Gardner Publications, 2000.

[63] B.J. Anderson, U.o.I.a. Urbana-Champaign, Rheology and Microstructure of Filled Polymer Melts, University of Illinois at Urbana-Champaign, 2008.

[64] P.J. Carreau, Rheological Equations from Molecular Network Theories, Transactions of the Society of Rheology, 16 (1972) 99-127.

[65] R.H. Colby, L.J. Fetters, W.W. Graessley, The melt viscosity-molecular weight relationship for linear polymers, Macromolecules, 20 (1987) 2226-2237.

[66] J.J. Cooper-White, M.E. Mackay, Rheological properties of poly(lactides). Effect of molecular weight and temperature on the viscoelasticity of poly(l-lactic acid), Journal of Polymer Science Part B: Polymer Physics, 37 (1999) 1803-1814.

[67] T.A. Osswald, Polymer Processing Fundamentals, Hanser, 1998.

[68] C. Barus, Note on the Dependence of Viscosity on Pressure and Temperature, Proceedings of the American Academy of Arts and Sciences, 27 (1891) 13-18.

SUPPORTING INFORMATION

High-pressure rheological analysis of CO_2-induced melting point depression and viscosity reduction of poly(ε-caprolactone)

S. Curia[a], D.S.A. De Focatiis[b], S.M. Howdle[a*]

A soaking time study showed that 15 minutes did not give a full CO_2 sorption. Repeating the experiments at longer times gave a lower T_m value.

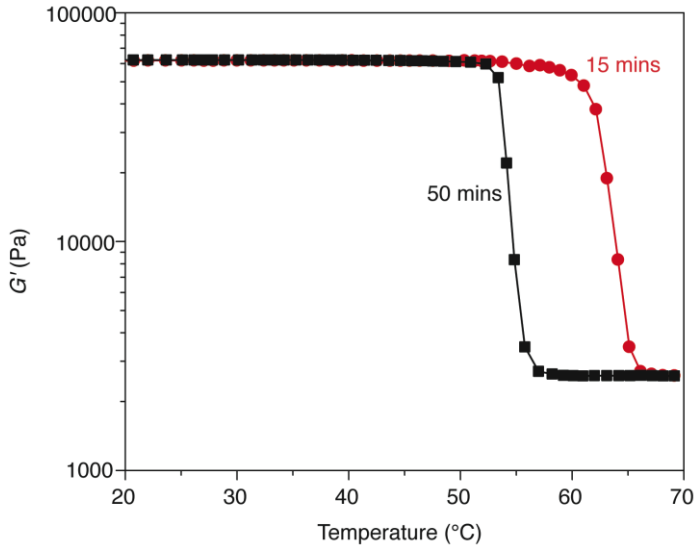

Fig. S- 1 - G' analysis on PCL10 over a range of temperatures at 70 bar and different soaking times: 15 minutes (red), 50 minutes (black).

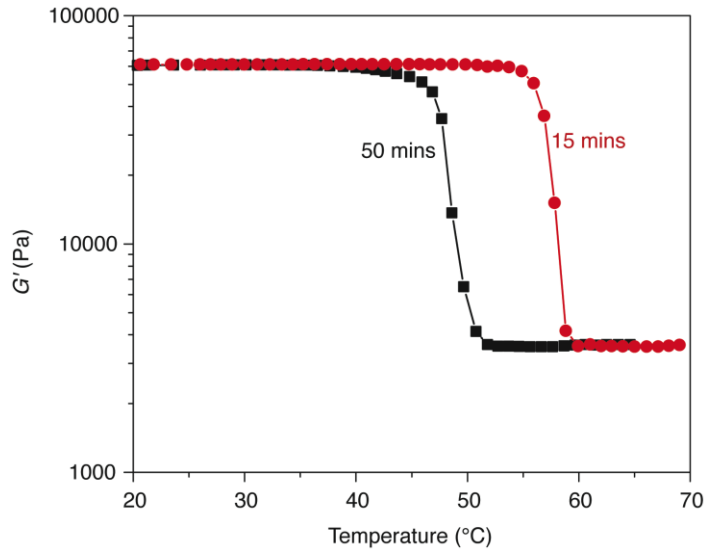

Fig. S- 2 - G' analysis on PCL10 over a range of temperatures at 100 bar and different soaking times: 15 minutes (red), 50 minutes (black).

After 50 minutes the results are reproducible and no further decrease was detected at longer times. Therefore, 50 minutes can be considered as an appropriate soaking time.

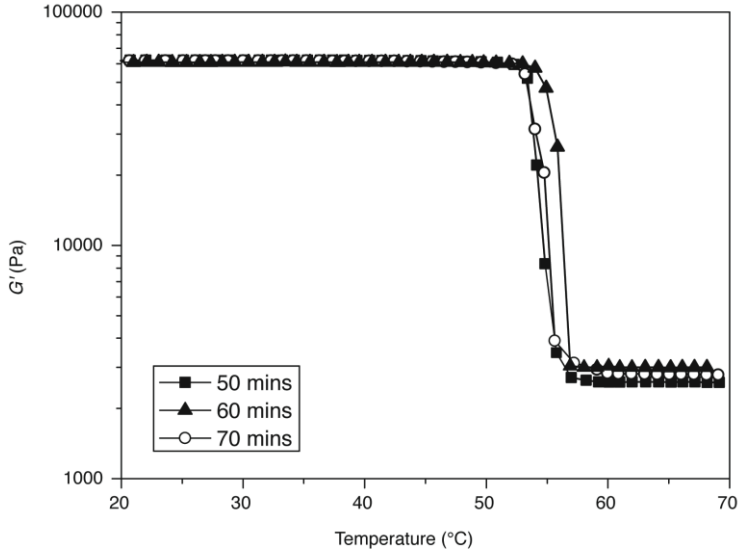

Fig. S- 3 - G' analysis on PCL10 over a range of temperatures at 70 bar and different soaking times: 50 minutes, 60 minutes and 70 minutes.

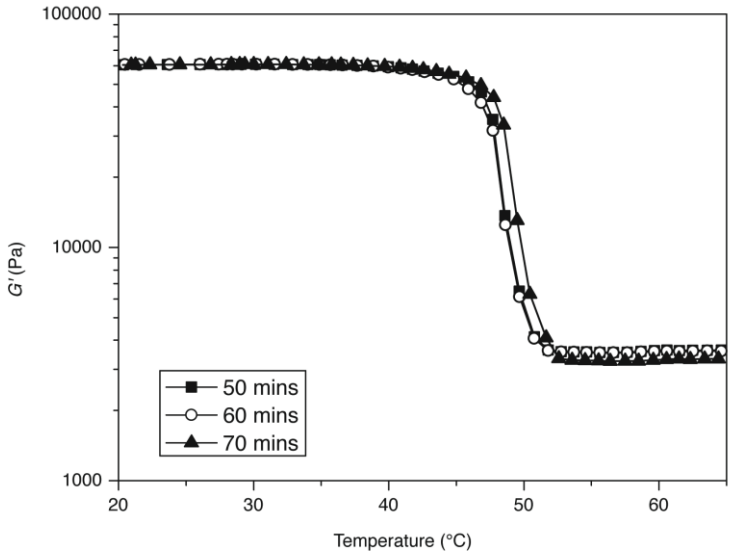

Fig. S- 4 - G' analysis on PCL10 over a range of temperatures at 100 bar and different soaking times: 50 minutes, 60 minutes and 70 minutes.

Similar results have been obtained with the view cell on a granular sample also in subcritical conditions, as shown below.

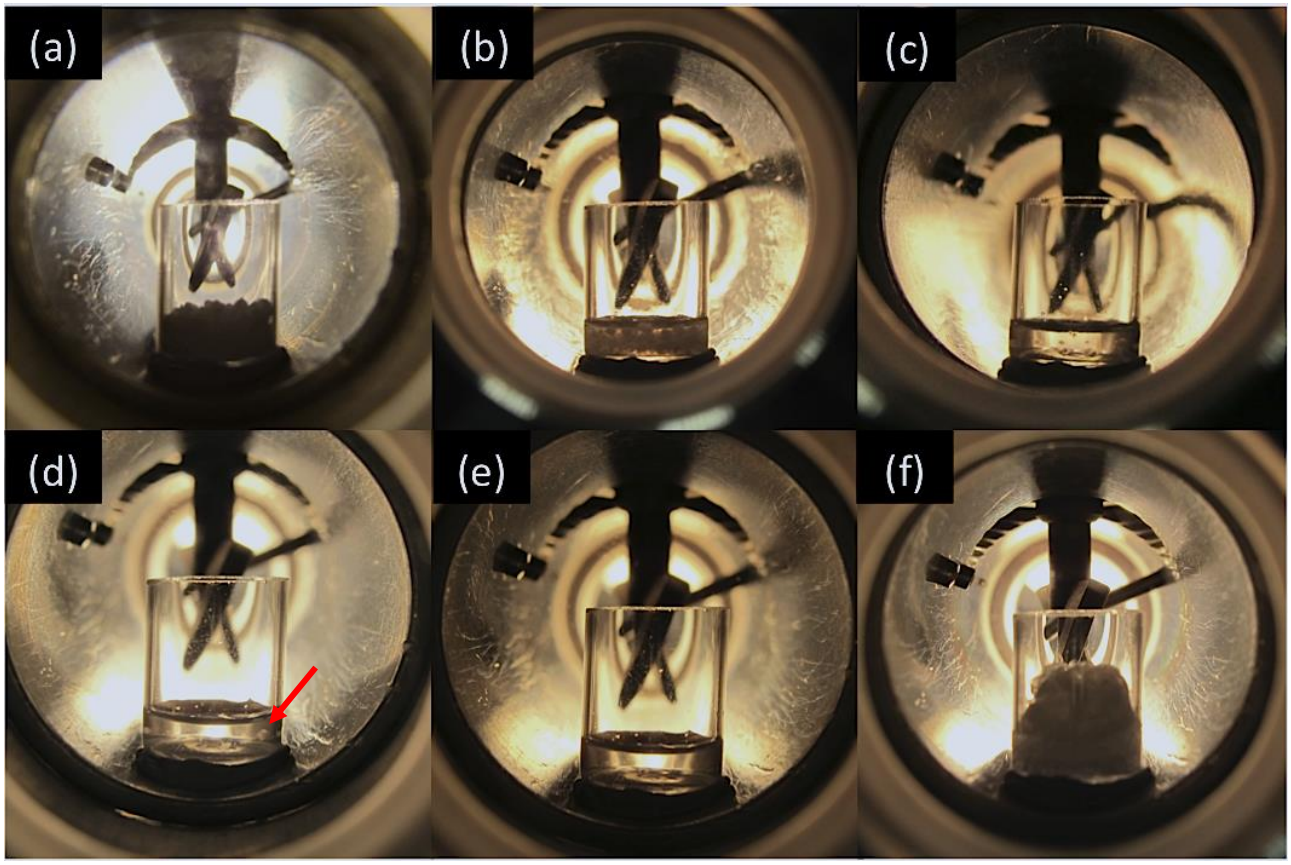

Fig. S- 5 - Transitions observed for PCL10 in the view cell under subcritical CO_2 (55 ^{o}C, 70 bar): (a) initial polymer in a granular form; (b) sample not fully plasticised after 25 minutes; (c) sample almost fully plasticised after 35 minutes; (d) sample after 45 minutes: few solid bits are still visible (red arrow); (e) after 48 minutes the sample is completely liquefied; (f) polymer foamed upon CO_2 removal.

Transient shear viscosity data at different shear rates shows that the CO_2-induced plasticisation mimics the temperature effects. The lack of any effects beyond the expected stress overshoots at high rates and linear viscoelasticity at low rates suggests that phase separation, solubility changes during shearing or bubble formation are unlikely to be taking place during the experiments.

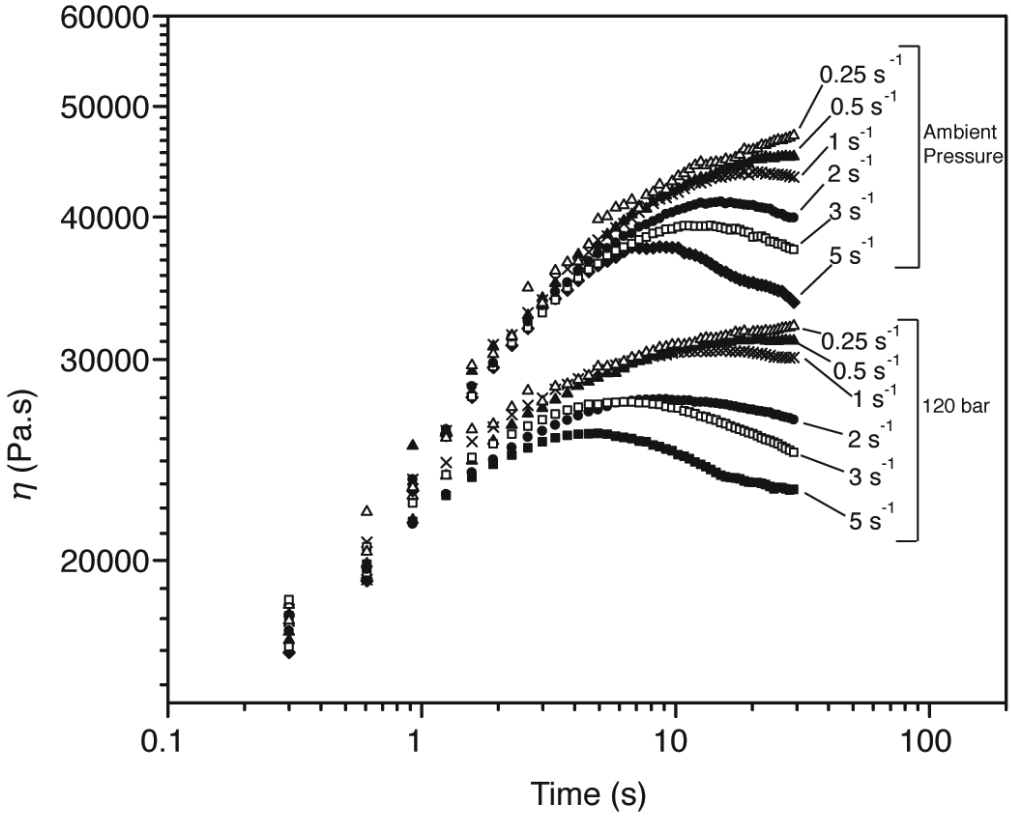

Fig. S- 6 – Transient shear viscosity *vs* time for PCL80 at 80 °C, at ambient pressure and under CO_2 (120 bar).

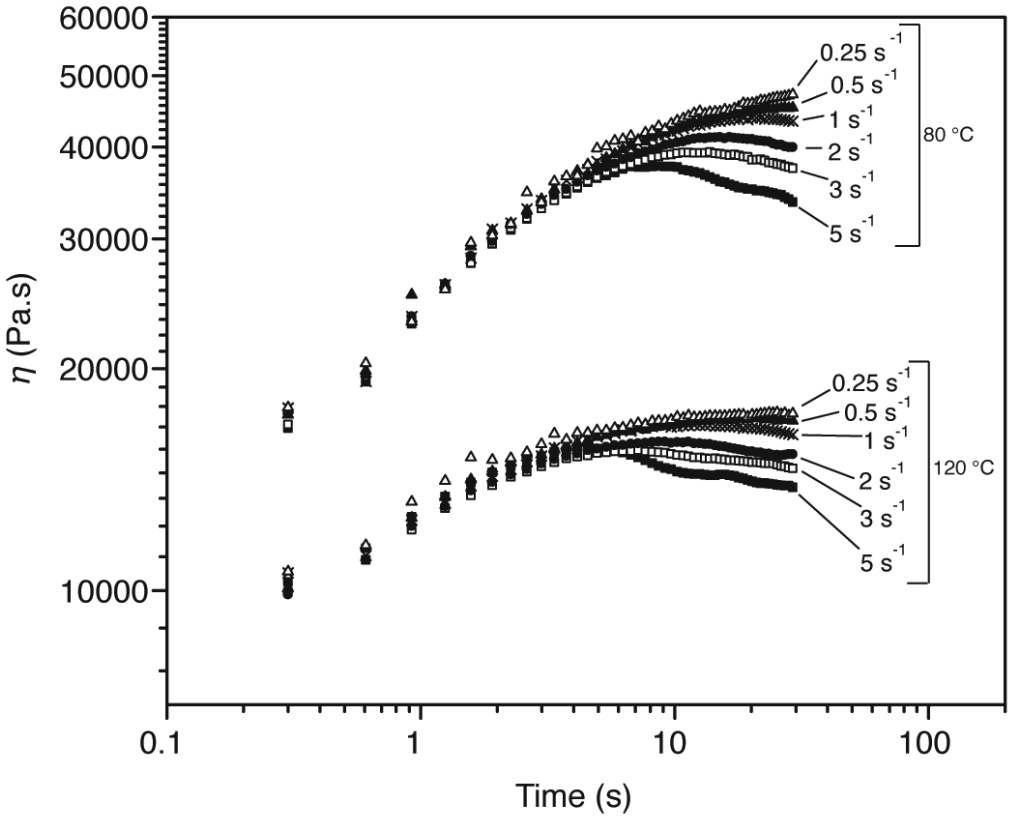

Fig. S- 7 - Transient shear viscosity *vs* time for PCL80 at 80 °C and 120 °C (ambient pressure) and under CO_2.

1